



# Characterization of Iodine-Related Molecular Processes in the Marine Microalga *Tisochrysis lutea* (Haptophyta)

Laura Hernández Javier<sup>1</sup>, Hicham Benzekri<sup>2</sup>, Marta Gut<sup>3,4</sup>, M. Gonzalo Claros<sup>2</sup>, Stefanie van Bergeijk<sup>5</sup>, José Pedro Cañavate<sup>5</sup> and Manuel Manchado<sup>5\*</sup>

<sup>1</sup> Programa de Genómica Evolutiva, Centro de Ciencias Genómicas, Universidad Nacional Autónoma de México, Cuernavaca, Mexico, <sup>2</sup> Departamento de Biología Molecular y Bioquímica, Universidad de Málaga, Málaga, Spain, <sup>3</sup> CNAG-CRG, Centre for Genomic Regulation, Barcelona Institute of Science and Technology, Barcelona, Spain, <sup>4</sup> Universitat Pompeu Fabra, Barcelona, Spain, <sup>5</sup> IFAPA Centro El Toruño, Junta de Andalucía, El Puerto de Santa María, Spain

## OPEN ACCESS

### Edited by:

Karla B. Heidelberg,  
University of Southern California,  
United States

### Reviewed by:

Julian Blasco,  
Consejo Superior de Investigaciones  
Científicas (CSIC), Spain  
Giovanna Romano,  
Stazione Zoologica Anton Dohrn, Italy

### \*Correspondence:

Manuel Manchado  
manuel.manchado@  
juntadeandalucia.es

### Specialty section:

This article was submitted to  
Aquatic Microbiology,  
a section of the journal  
Frontiers in Marine Science

**Received:** 13 January 2018

**Accepted:** 04 April 2018

**Published:** 24 April 2018

### Citation:

Hernández Javier L, Benzekri H,  
Gut M, Claros MG, van Bergeijk S,  
Cañavate JP and Manchado M (2018)  
Characterization of Iodine-Related  
Molecular Processes in the Marine  
Microalga *Tisochrysis lutea*  
(Haptophyta). *Front. Mar. Sci.* 5:134.  
doi: 10.3389/fmars.2018.00134

Iodine metabolism is essential for the antioxidant defense of marine algae and in the biogeochemical cycle of iodine. Moreover, some microalgae can synthesize thyroid hormone-like compounds that are essential to sustain food webs. However, knowledge regarding iodine-related molecular processes in microalgae is still scarce. In this study, a *de novo* transcriptome of *Tisochrysis lutea* cultured under high iodide concentrations (5 mM) was assembled using both long and short reads. A database termed IsochrysisDB was established to host all genomic information. Gene expression analyses during microalgal growth showed that most of the antioxidant- (*aryl*, *ccp*, *perox*, *sod1*, *sod2*, *sod3*, *apx3*, *ahp1*) and iodide-specific deiodinase (*dio*) genes increased their mRNA abundance progressively until the stationary phase to cope with oxidative stress. Moreover, the increase of *dio* mRNA abundance in aging cultures indicated that this enzyme was also involved in senescence. Cell treatments with iodide modified the expression of *perox* whereas treatments with iodate changed the transcript levels of *gpx1* and *ccp*. To test the dependence of *perox* on iodide, microalgae cells were treated with hydrogen peroxide (H<sub>2</sub>O<sub>2</sub>) either in presence or absence of iodide observing that several genes related to reactive oxygen species (ROS) deactivation (*perox*, *gpx1*, *apx2*, *apx3*, *ahp1*, *ahp2*, *sod1*, *sod3*, and *aryl*) were transcriptionally activated although with some temporal differences. However, only the expression of *perox* was dependent on iodide levels indicating this enzyme, acquired by horizontal gene transfer (HGT), could act as a haloperoxidase. All these data indicate that *T. lutea* activates coordinately the expression of antioxidant genes to cope with oxidative stress. The identification of a phase-regulated deiodinase and a novel haloperoxidase provide new clues about the origin and evolution of thyroid signaling and the antioxidant role of iodine in the marine environment.

**Keywords:** hydrogen peroxide, iodide, *Tisochrysis lutea*, peroxidase, deiodinase, gene expression

## INTRODUCTION

Phytoplankton is responsible for approximately half of the atmospheric oxygen through oxygenic photosynthesis and provides food resources to sustain the vast majority of marine life (Falkowski, 2012; Chapman, 2013). Along evolution, oxygenic photosynthesis created an oxygen-rich environment that generated high toxic reactive oxygen species (ROS) which are prone to damage functional macromolecules including DNA, proteins and structural lipids (Yilancioglu et al., 2014). Aside of exogenous ROS sources, several endogenous metabolic pathways in microalgae produce ROS including hydrogen peroxide ( $H_2O_2$ ) as a by-product of glycolate recycling and fatty acid oxidation in the peroxisome and superoxide ( $O_2^{\cdot-}$ ) during oxidative phosphorylation in the mitochondria and photosynthesis via the Mehler reaction in the chloroplast (Cirulis et al., 2013). To detoxify ROS and preserve cellular homeostasis, microalgae have developed a wide range of protective mechanisms including ROS-specific antioxidant enzymes and low molecular weight ROS scavengers. With respect to the enzymes, the most important are superoxide dismutases (SODs) which remove  $O_2^{\cdot-}$  by dismutation into  $H_2O_2$ , and peroxidases that catalyze the reduction of  $H_2O_2$  to water. Among scavenging molecules, polyphenols, pigments, ascorbate, glutathione, and some halogenated metabolites including iodide appear as the most important chemical ROS scavengers to prevent oxidative injury (Cirulis et al., 2013; Gribble, 2015).

In marine environments, iodide is considered as the most ancient and powerful mechanism against ROS (Venturi and Venturi, 1999; Venturi, 2011). Küpper et al. (2008) demonstrated that macroalgae accumulate iodide as an antioxidant mechanism that can rapidly and non-enzymatically scavenge ROS (i.e.,  $O_3$ ,  $O_2$ ,  $^1O_2$ , and  $OH^{\cdot}$ ), or can act as an electron donor for haloperoxidase enzymes to degrade  $H_2O_2$ . Moreover, this enzyme has been revealed as critical for extracellular iodide uptake thanks to iodine oxidation to hypoiodous acid as a previous step to cell membrane diffusion. One part of the iodine is transformed to volatile halocarbons responsible for the maintenance of the geochemical functioning of the global iodine. Another iodine fraction is intracellularly reduced to iodide or iodinated to organic substrates that act as antioxidant defense reservoirs to scavenge ROS or against excessive predation (Küpper et al., 1998; Gribble, 2003; Iwamoto and Shiraiwa, 2012). The most common organic forms of iodine in algae (that can comprise up to 1% iodine by weight) are iodomethane ( $CH_3I$ ) and its derivatives. In this regard, it is worth noting that some algae are able to accumulate iodotyrosine-derived compounds including monoiodotyrosine (MIT), diiodotyrosine (DIT), triiodothyronine ( $T_3$ ), and thyroxine ( $T_4$ ) (Chino et al., 1994; Heyland and Moroz, 2005; La Barre et al., 2010; Taylor and Heyland, 2017). The spontaneous reaction between tyrosine and iodine to synthesize MIT and DIT reported in some eukaryotic phyla is believed to occur spontaneously (Crockford, 2009; La Barre et al., 2010). This reaction is involved in cell-to-cell endocrine communication and it is also critical for consumers to sustain developmental processes such as the larval metamorphosis of marine invertebrates. Metabolic functions

associated to oxidative stress can thus be involved in the origin and evolution of thyroid regulatory pathways in deuterostomes (Laudet, 2011; Taylor and Heyland, 2017). Despite the important antioxidant function of iodide in the algae and its qualitative role to sustain development of key organisms in main food webs, mechanisms related with iodide metabolism are poorly understood in microalgae.

*Tisochrysis lutea*, previously named *Isochrysis aff. galbana* (Clone Tahiti) (Bendif et al., 2013) is a small haptophyte within the class Coccolithophyceae. This microalga is widely used in aquaculture due to its high content in polyunsaturated fatty acids, particularly in docosahexaenoic acid (DHA, 22:6n-3) that can reach 8–10% of total fatty acids (Guedes and Malcata, 2012; Rasdi and Qin, 2015). Hence, this microalga has become very popular in most hatcheries for fish and invertebrate larval production as well as for the extensive production of bivalves (Guedes and Malcata, 2012). In addition to its nutritional value, *T. lutea* is a microalga that accumulates thyroid hormone (TH)-like compounds (Heyland and Moroz, 2005), indicating a particular iodide-related metabolism, what confers novel functional characteristics. Previous data of our group demonstrated this microalga is able to incorporate iodide from the environment after oxidation by enzymatic (haloperoxidase-mediated) or non-enzymatic ways (catalyzed by iron) (van Bergeijk et al., 2013, 2016). Moreover, a fraction of intracellular iodine is organified as TH-like hormones (Heyland and Moroz, 2005). However, iodine is not essential for growth in *T. lutea* (Iwamoto and Shiraiwa, 2012; van Bergeijk et al., 2016) suggesting this element could exert other functions such as that of antioxidant defense. The identification of a putative haloperoxidase involved in iodine organification as well as putative deiodinases controlling iodine mobilization will be important to better understand iodine metabolism and its function in this microalga.

Four different types of haloperoxidases are currently considered in a wide range of organisms including brown algae, red algae, gram-negative bacteria, fungi, and some invertebrates (Gwon et al., 2014). In *Laminaria digitata*, the haloperoxidases play a key role in the specific uptake of iodide from seawater and nucleotide sequences encoding for vanadium iodoperoxidases were reported (Colin et al., 2005; Leblanc et al., 2006; Verhaeghe et al., 2008). In microalgae, some studies reported haloperoxidase activity (Moore et al., 1996; Murphy et al., 2000; Hill and Manley, 2009; Hughes and Sun, 2016), however, putative genes encoding putative iodoperoxidases have not been identified to date. Moreover, iodotyrosine deiodinases were only described in metazoan and bacteria (Phatarphekar et al., 2014; Taylor and Heyland, 2017) and iodothyronine deiodinases were restricted to metazoa and between social amoebae (Lobanov et al., 2007; Orozco et al., 2012; Singh et al., 2014). To increase the knowledge about iodine metabolism and oxidative defenses in *T. lutea*, the aims of this study were: (i) *de novo* assembly and characterization of a transcriptome for *T. lutea* cultured at high iodide concentrations; (ii) To quantify the expression patterns of antioxidant- and iodine-related genes during growth; (iii) To quantify the expression patterns of selected genes in response to iodide and iodate treatments (iv) To quantify the

expression patterns of selected genes in response to H<sub>2</sub>O<sub>2</sub> and iodide treatments. Results represent new important clues about the emergence of deiodinases and TH signaling in the marine environment as well as the identification of a novel functional haloperoxidase acquired by horizontal gene transfer (HGT).

## MATERIALS AND METHODS

### Microalgal Strain

The marine microalga *T. lutea*, was purchased from the Culture Collection of Algae and Protozoa in Oban, Scotland (CCAP 927/14). Stock cultures were treated with a mix of streptomycin (50 mg l<sup>-1</sup> final concentration) and ampicillin (250 mg l<sup>-1</sup> final concentration) or with chloramphenicol (35 mg l<sup>-1</sup> final concentration) to remove any bacterial contamination. The lack of bacteria was checked microscopically and by plating on Marine Agar 2216 (Difco). Cultures were grown and maintained in an illuminated incubator (Sanyo MLR-351) at 20°C and an irradiance of 50 μmol photons m<sup>-2</sup> s<sup>-1</sup>. Standard stock cultures (vol 0.35 L) were carried out in 0.5 L by weekly transferring sterile artificial seawater (ASW; salinity 35 and pH 8.0) with f/2 nutrients as previously described (van Bergeijk et al., 2016).

### Experimental Set-Up

#### Growth Conditions and Culture Media

Microalga cultures were carried out in a temperature-controlled room (20°C) under continuous illuminating conditions using a cool white fluorescent light (100 μmol photons m<sup>-2</sup> s<sup>-1</sup>). These conditions are considered optimal to ascertain less variable redox conditions with an optimal quantum yield (Fv/Fm) kept at maximum values (van Bergeijk et al., 2016). Cultures were bubbled with filter-sterilized air (Acro 50 Vent devices, 0.2 μm PTFE, Pall Corporation) enriched with 1% CO<sub>2</sub>. All cultures were carried out using autoclaved ASW enriched with filter-sterilized f/2 nutrients (0.5 mM N) as previously described (van Bergeijk et al., 2016). All manipulations of the cultures were aseptically carried out in a laminar flow hood.

To evaluate expression patterns during microalga growth, three replicate cultures in 5L-flasks containing 5 L of medium were grown for 17 days under the conditions described above. Replicate flasks were inoculated with starting cultures to obtain an initial cell density of 0.5 × 10<sup>6</sup> cells ml<sup>-1</sup>. Daily, each flask was sampled for cell density and gene expression analyses. Cell density was estimated in samples fixed with Lugol's fixative. For gene expression, cells (~2 × 10<sup>8</sup>) were harvested by centrifugation at 4,083 × g for 10 min and 4°C. Pellets were washed in autoclaved ASW and then centrifuged at 5,900 × g for 5 min at 4°C. The cell pellets were stored at -80°C until analysis.

To evaluate the effect of iodide (I<sup>-</sup>) and iodate (IO<sub>3</sub><sup>-</sup>) on gene expression, nine 2-L flasks containing 1.5 L of medium were inoculated with *T. lutea* and cultivated for 4 days (exponential phase) under the above conditions. Three flasks were added potassium iodide (final concentration 5 mM; Sigma-Aldrich) and other three flasks were added potassium iodate (5 mM; Sigma-Aldrich), whereas the remaining three flasks were kept as the untreated control group. Microalgae were harvested at 3 and

6 h after the treatments. The samples were collected as indicated above and kept at -80°C until analysis.

To evaluate the effect of H<sub>2</sub>O<sub>2</sub> and iodide on gene expression, one 2-L flask containing 1.5 L medium was inoculated with *T. lutea* (initial density 0.5 × 10<sup>6</sup> cells ml<sup>-1</sup>) and grown for 4 days (in exponential phase) under the same conditions reported above. Then, this culture was split into twenty-four 50-mL flasks containing 40 mL of culture. Half of flasks were firstly added iodide (0.5 mM final concentration). Then, half of I<sup>-</sup>-added and half of non-I<sup>-</sup> added flasks were treated with H<sub>2</sub>O<sub>2</sub> (200 μM; Sigma-Aldrich). Microalgae were harvested at 5 and 45 min after H<sub>2</sub>O<sub>2</sub> addition by centrifuging at 6,000 × g for 5 min and 5°C. H<sub>2</sub>O<sub>2</sub> was immediately measured in the supernatant. The pellets were kept at -80°C until analysis.

### Biological Culture Parameters

#### Cell density

Microalgae cell densities determined with the hemocytometer were used to calculate the specific growth rate was according to the equation:  $\mu = (\ln N_t - \ln N_0) / (t - t_0)$ , where N<sub>0</sub> is the cell number at the start of the exponential phase (t<sub>0</sub>), and N<sub>t</sub> is the cell number at time t of the exponential phase.

#### Hydrogen peroxide quantification

The concentration of extracellular H<sub>2</sub>O<sub>2</sub> was measured colorimetrically using the Quantitative Peroxide Assay Kit (Prod No. 23285; Thermo Scientific). In this assay hydrogen peroxide converts Fe<sup>2+</sup> to Fe<sup>3+</sup> at acidic pH, which complexes with a xylenol orange dye to yield a purple product with maximum absorbance at 560 nm. Samples were measured in a spectrophotometer against a calibration curve of H<sub>2</sub>O<sub>2</sub> in ASW, which was linear up to 100 μM. When needed, samples were diluted with ASW before analysis.

### Transcriptome Sequencing and Characterization

Total RNA was isolated using the RNeasy Plant Mini Kit (Qiagen) according to the manufacturer's instructions. Before sequencing, RNA integrity was checked using the Bioanalyzer 2100 (Agilent Technologies). To achieve a good transcript representation and assembly, both long (454 Roche) and short (Illumina) reads were generated using different microalgal samples and methodological approaches. In the case of long-reads, six 0.5-L flasks containing 0.4 L of ASW enriched with f/2 nutrients were inoculated with *T. lutea* (initial cell density of 0.5 × 10<sup>6</sup> cells ml<sup>-1</sup>) and cultivated for 4 days. Three flasks were added chloramphenicol (35 mg l<sup>-1</sup> final concentration) and all of them were added potassium iodide (5 mM final concentration). At the fourth day, microalgae (~2 × 10<sup>8</sup> cells) were harvested by centrifugation at 4,083 × g for 10 min at 4°C. Pellets were washed in autoclaved ASW, transferred to 1.5-mL tubes and then centrifuged at 5,900 × g for 5 min at 4°C. The cell pellets were stored at -80°C until analysis. Total RNA from *T. lutea* samples grown without chloramphenicol was isolated as indicated below. For sequencing, the three biological replicates were pooled in the same proportion and cDNA normalized using the SMART technology. In the case of microalgae cultivated with chloramphenicol, total RNA from the three biological replicates was also pooled and the cDNA



was not normalized but the most abundant bands visible by electrophoreses corresponding to chloroplast sequences were cut and removed before 454 libraries preparation. These samples were sequenced by 454/Roche technology as previously described (Benzekri et al., 2014).

For the generation of the transcriptomic short-reads, two types of Illumina libraries were prepared. Firstly, a pool of total RNA from microalgae cultivated with chloramphenicol and potassium iodide, as indicated above for long-read sequencing, was normalized using the Mint Universal (Evrogen) and Trimmer (Evrogen) kits and libraries were constructed using the TruRNA-Seq kitv2. Secondly, seven samples of the experiment described above to evaluate the effect of H<sub>2</sub>O<sub>2</sub> and iodide on gene expression were selected: untreated control at 5 and 45 min, I<sup>-</sup>-added (0.5 mM) samples at 5 and 45 min, I<sup>-</sup>- and H<sub>2</sub>O<sub>2</sub>-added (200 μM) samples at 5 and 45 min and sample H<sub>2</sub>O<sub>2</sub>-added at 5 min. The three biological replicates of each condition (~2 × 10<sup>8</sup> cells at 4 day of culture) were equally pooled and seven cDNA libraries were prepared using the mRNA-Seq sample preparation kit as previously described (Benzekri et al., 2014).

### Bioinformatic Analysis

Raw data were processed and assembled at the Plataforma Andaluza de Bioinformática (PAB). The strategy for transcriptome assembly is indicated in Supplementary data sheet 1. Roche/454 long-reads and Illumina short-reads were pre-processed using the SeqTrimNext pipeline (<http://www.scbi.uma.es/seqtrimmex>; Falgueras et al., 2010), available at the PAB using the specific NGS technology configuration parameters. Long-reads were assembled using MIRA3 (Chevreux et al., 2004) and EULER-SR (Pevzner et al., 2001) with the default parameters and a *k*-mer = 29 (maximum length allowed). Contigs obtained were mapped onto the original reads using Bowtie (Langmead and Salzberg, 2012) allowing two mismatches to confirm the goodness of the final consensus. Unmapped contigs were considered a sign of misassembly and were submitted to Full-LengtherNext (Seoane et al., in preparation) analysis to recover putative coding sequences.

The Illumina short-reads were assembled with SOAP *de novo* (Luo et al., 2012) using two *k*-mers (23 and 47) since the use of multiple *k*-mers is reported to improve the quality and good performance of *de novo* assembly (Surget-Groba and Montoya-Burgos, 2010). Processed single reads and paired reads were assembled independently. Thereafter, a script was used to discard misassembled contigs based on the presence of exact, internal, direct or inverse repetitions. Preassemblies were finally reconciled using CAP3 with default parameters to provide the maximal set of transcripts that resulted in *T. luteav1* transcriptome. To avoid contaminant sequences due to the sequencing depth used, a BLAST comparison was carried out with the *T. lutea* transcriptome previously described by Carrier et al. (2014). Those transcripts only represented in *T. luteav1* transcriptome with a low number of reads mapped (<10 reads by transcript) with annotation hits for other organisms like *H. sapiens* or fish species were considered as sequence contamination and removed to generate the *T. luteav2* transcriptome.

Transcripts were annotated using Sma3s (Muñoz-Mérida et al., 2014), AutoFact and Full-LengtherNext filtering for  $E < 10^{-10}$  and a minimal identity of 30% as reported in Benzekri et al. (2014). The homology identification analysis was performed using Blastx at NCBI database. All proteins with  $E < 10^{-6}$  and an identity  $\geq 25\%$  were considered.

For phylogenetic analysis, a set of sequences encoding for deiodinases in metazoans was retrieved from GenBank/EMBL/DDBJ and SoleaDB (Benzekri et al., 2014) databases (Accession numbers are shown in Supplementary data sheet 2). Sequences were aligned using ClustalV methods implemented in Megalign (Dnastar). Maximum likelihood (ML) phylogenetic analysis was carried out using ProtTestv3.2 and the PHYLIP package. The best-fit model for sequence evolution was JTT+I+G+F. A tree was drawn using Figtree v1.4.2 (<http://tree.bio.ed.ac.uk/software/figtree/>). Sequence names used in the phylogeny are indicated in Supplementary data sheet 2.

### RNA Isolation and Gene Expression Analysis

Homogenization of microalgal cells was carried out using Lysing Matrix D (MP Biomedicals) for 40 s at speed setting 6 in the Fastprep FG120 instrument (Bio 101). Total RNA was extracted from frozen samples using the RNeasy Plant Mini Kit (Qiagen) according to the manufacturer's instructions. In all cases, total RNA was treated twice with DNase I using the RNase-Free DNase Kit (Qiagen) to avoid amplification of contaminated genomic DNA. RNA sample quality was assessed by electrophoresis and quantification was performed spectrophotometrically (NanoDrop 8000). Total RNA (1 μg) from each sample was reverse-transcribed using the iScript™ cDNA Synthesis kit (Bio-Rad).

Real-time analysis was carried out on an iCycler (Bio-Rad). Reactions were performed in a 10 μl volume containing cDNA generated from 10 ng of original RNA template, 300 nM each of specific forward and reverse primers, and 5 μl of Mix SYBR Premix Ex Taq™ (Takara). Matching oligonucleotide primers were designed using Oligo v6.89 software (Medprobe) (Table 1). The amplification protocol used was as follows: initial 15 min denaturation and enzyme activation at 95°C, 40 cycles of 95°C for 30 s, 68°C for 15 s, and 72°C for 1 min. Each assay was performed in duplicate. For normalization of cDNA loading, all samples were run in parallel using the elongation factor (*ef1a*) and ubiquitin (*ubi*) as reference genes but only the latter was used due to its higher stability. Relative mRNA expression was determined using the  $2^{-(\Delta\Delta Ct)}$  method. Data were calibrated to the first day of culture in microalgal growth experiment, to the untreated control in the iodide and iodate experiment and to the 5 min control samples added iodide but not hydrogen peroxide.

### Statistical Analysis

All data were checked for normal distribution with the Kolmogorov–Smirnov test as well as for homogeneity of the variances with the Levene's test and when necessary, log transformation was applied. A simple ANOVA was used to test significant differences along the growth curves. Moreover, a General Linear Model (GLM) analysis using time, H<sub>2</sub>O<sub>2</sub> and

**TABLE 1** | Primers used for qPCR analyses.

| Gene product                  | Gene name    | Amplicon (pb) | Access no     | Primer (5'→3')  |
|-------------------------------|--------------|---------------|---------------|---|
| Elongation factor 1a          | <i>eef1a</i> | 125           | unigene32269  | (f) ACAAGAAGCGCGGTACGACGAGGT<br>(r) GTCGCCCATCCAGCCGGAGA          |
| Ubiquitin                     | <i>ubi</i>   | 79            | unigene658    | (f) GGTGTGATCGAGCCGTCGCTTG<br>(r) GCGCATAGCAGATCCGGCACACCT        |
| Deiodinase                    | <i>deio</i>  | 73            | unigene33536  | (f) ACGATGTCAAACACGCGCAGACCC<br>(r) ATGTGCGATCCGCTGACAACTTGCT     |
| Superoxide dismutase1         | <i>sod1</i>  | 105           | unigene33773  | (f) CAAGGTGGATACAGCCAGCGGCAT<br>(r) TCATACGTGAGACCAACGGCCCAT      |
| Superoxide dismutase2         | <i>sod2</i>  | 105           | unigene572    | (f) GCTCGCCGACGGCAGCCTTT<br>(r) CCCTCCAGATTGGTGAGCGCGAC           |
| Superoxide dismutase3         | <i>sod3</i>  | 69            | unigene144078 | (f) GATCTTGACAGAGCCGTCCTTGGTGA<br>(r) CAGTTCTCCACCGCGCTGCT        |
| Cytochrome c peroxidase       | <i>ccp</i>   | 96            | unigene34360  | (f) CGTGGACTCTGAAGGAATGGGACGG<br>(r) TGTCTTGGATCAGGGCAATGTCGG     |
| Glutathion peroxidase 1       | <i>gpx1</i>  | 80            | unigene33605  | (f) CGTGCAACCAGTTCGGCCACC<br>(r) AGCAGTCCGCCAGGCAAC               |
| Putative arylesterase         | <i>aryl</i>  | 70            | unigene33427  | (f) CAAAAGTGATGCAAGACCATGCGAAG<br>(r) AGAGCCGGTACTGTGATACGAGGCAGA |
| Ascorbate peroxidase2         | <i>apx2</i>  | 124           | unigene34311  | (f) CCACTGACAATGCGCTCAAGACGGA<br>(r) CAGCCGAGCGAGAGGAGGCGTTC      |
| Ascorbate peroxidase3         | <i>Ap3</i>   | 97            | unigene27544  | (f) TCCCGATGGACTTCTTGGAGCA<br>(r) GTGTGAGCACCGGAGAGCGCAAC         |
| Peroxidase                    | <i>perox</i> | 82            | unigene21650  | (f) TTGACTCTCCGATTTTGCGAAGGCTA<br>(r) ACCAGAACGAGAGCCAGGGGAAC     |
| Alkyl-hydroperoxide reductase | <i>ahp1</i>  | 111           | unigene909    | (f) CTGCTCAAACGACCCGGTGGAG<br>(r) GCTGCATGGTAGGCGACGCTGA          |
| Alkyl-hydroperoxide reductase | <i>Ahp2</i>  | 66            | unigene36849  | (f) GCGCACGATGCTTGAGGTACGGT<br>(r) GGGCATGGGTGGCGAAAGCTCT         |

Gene product and name, accession number at IsochrysisDB *T.luteav2* and forward (f) and reverse (r) primers are shown.

iodide levels as fixed factors was carried out to test significant differences associated with these treatments.

## RESULTS

### De Novo Sequencing of *T. lutea* Transcriptome

The transcriptome of *T. lutea* cultivated under different iodide and hydrogen peroxide conditions was sequenced using long- (454) and short-reads (Illumina). A total of  $1.6 \times 10^6$  and  $1,539 \times 10^6$  of raw sequence reads, were generated respectively (Supplementary data sheet 1) and deposited in the BioProject PRJNA418294. Intriguingly, data pre-processing showed that normalized libraries resulted in the highest levels of redundant sequences (66.2–68.3%) mainly originating from chloroplasts. The main characteristics of the assembled transcriptomes are depicted in **Table 2** and Supplementary data sheet 1. Assembly of long reads ( $0.72 \times 10^6$  of clean sequences) generated 23,405 transcripts with 52.2% longer than 500 bp (**Table 2**). When both long and short reads were jointly processed (*T. luteav2* assembly), the total number of transcripts increased to 69,800

(50.9% longer than 500 bp), with 23.2% representing different complete open reading frames (ORFs) and 47.6% different gene orthologs. To reduce transcript redundancy (splicing forms and partial sequences encoding the same gene) in the full transcriptome, Full-LengtherNext was used to select a subset of unique sequences (23,671) to build a reference transcriptome. *In silico* Blastx comparisons between the reference transcriptome and the transcriptomic information previously reported by Carrier et al. (2014) for this microalga demonstrated a matching of 98.7% (sequence alignment >95% and cut-off *E*-value  $<1.0E^{-10}$ ; Supplementary Table 1). A total of 16,363 sequences perfectly matched (100%) between both transcriptomes. For the full transcriptome, the matching correspondence with Carrier's transcriptome ranged between 89.3 and 92.0% (Supplementary Table 1).

Annotation percentages were 42.4 and 57.0% for the full and reference transcriptomes, respectively. Gene Ontology analysis showed that categories were equally represented in both transcriptomes with catalytic activity (51.1%), cellular (38.4%), and cellular process (28.6%) as the most represented ones in the molecular function, cellular component and biological process domains, respectively (Figure S1). KEGG analysis indicated that

**TABLE 2** | Overview of quality parameters for assembled long-reads (454 transcripts) and final *T.luteav2* transcriptome.

|   | 454 Transcripts |      | <i>T. luteav2</i> |      |
|---|-----------------|------|-------------------|------|
|   | N               | %    | N                 | %    |
| Artifacts <sup>a</sup>                    | 425             |      | 3,339             | 4.6  |
| Valid transcripts                         | 23,405          |      | 69,800            | 100  |
| >500 pb                                   | 12,205          | 52.2 | 36,360            | 50.9 |
| >200 pb                                   | 20,277          | 86.6 | 50,035            | 71.7 |
| Longest unigene                           | 7,729           |      | 10,309            | –    |
| Transcripts with ortholog <sup>b</sup>    | 10,502          | 44.9 | 23,939            | 34.3 |
| Different ortholog IDs                    | 7,816           | 74.4 | 11,392            | 47.6 |
| Complete ORFs                             | 1,796           | 17.1 | 9,199             | 38.4 |
| Different, complete ORFs                  | 1,625           | 15.5 | 5,546             | 23.2 |
| C-terminus                                | 4,217           | 18.0 | 6,661             | 9.5  |
| N-terminus                                | 930             | 4.0  | 2,764             | 4.0  |
| Internal                                  | 3,559           | 15.2 | 5,315             | 7.6  |
| Putative ncRNA                            | 7               | 0.03 | 27                | 0.04 |
| Transcripts without ortholog <sup>b</sup> | 12,896          | 55.1 | 45,834            | 65.7 |
| Putative new transcripts                  | 6,939           | 53.8 | 19,645            | 42.9 |
| Unknown                                   | 5,957           | 25.5 | 26,189            | 57.1 |
| Reference transcriptome                   |                 |      | 23,671            |      |

Full strategy for transcriptome assembly is depicted in Data sheet S1. Statistical data and the minimum number of transcripts to build the reference transcriptome were obtained by using Full-LengtherNext.

<sup>a</sup>Artifacts refer mainly to misassemblies and chimeric contigs.

<sup>b</sup>Percentages for subclassifications of this category were calculated using this line as 100% reference.

all major metabolic pathways were represented and a total of 1,757 transcripts could be assigned to at least one known universal KEGG pathway.

All transcriptomic information generated in this study was hosted at IsochrysisDB (<http://www.scbi.uma.es/isochrysisdb/>). This database was built, structured and designed in a user-friendly manner showing all information regarding experimental conditions, information about NGS libraries and processing bioinformatics pipelines to clean, assemble and annotate these transcriptomes. In the “All Assemblies” tab, the different assembly versions can be browsed. In the “Unigenes” section, users can search for specific transcripts and browse specific information about annotation, ORF prediction, and putative markers (Figure 1). Moreover, transcripts can be browsed for SNPs, SSRs, Descriptions, GOs, EC, KEGGs, and InterPros annotations.

## Identification of Transcripts Related to Antioxidant Defenses and Iodide Metabolism

Several searches using key terms were carried out at IsochrysisDB and three SODs (*sod1*, *sod2*, and *sod3*), some peroxidases including the cytochrome c peroxidase (*ccp*), one glutathione peroxidase (*gpx1*), one putative peroxidase (*perox*), and two ascorbate peroxidases (*apx2* and *apx3*), two alkyl-hydroperoxide

reductases (*ahp1* and *ahp2*), one arylesterase (*aryl*), and one iodothyronine deiodinase (*dio*) were identified (Supplementary Table 2; *E*-value <1.0E-06). The annotation was further confirmed by BLASTx at NCBI (Supplementary Table 2). Analysis of homologous transcripts in bacteria, fungi, plants and vertebrates showed a high number of conserved domains in all of them except in *perox* (Table 3 and Supplementary data sheet 3) with only 18 similar sequences in ciliates, amoeba, bacteria, and dinoflagellates. The best hit with annotation showed an *E*-value < 10<sup>-17</sup> and a putative peroxidase function of *Oxytricha trifallax* (EJY77502) (Table 3).

About conserved domains, *sod1* and *sod2* appeared as Cu,Zn SOD *sod3* as Mn-Fe SOD (Table 3). The peroxidase domain was identified in *ccp*, *apx2*, *apx3*, and *perox* genes and the *aryl* appeared as alpha/beta-hydrolase. Moreover, a thioredoxin domain was found in transcripts such as *gpx1*, *ahp1*, *ahp2*, and *dio*. This latter was highly homologous of type I iodothyronine deiodinase in vertebrates (Supplementary data sheet 2). A search for SeCIS elements confirmed the presence in the putative sequence *gpx1* but failed in the *dio* encoding sequence one. A phylogenetic analysis of *dio* with homologous in invertebrates and vertebrates indicated that this deiodinase clustered separately for their counterparts indicating its ancestral origin (Figure 2). Moreover, a Cys residue instead of SeCys highly conserved in vertebrates was found in the active site (Supplementary data sheet 2).

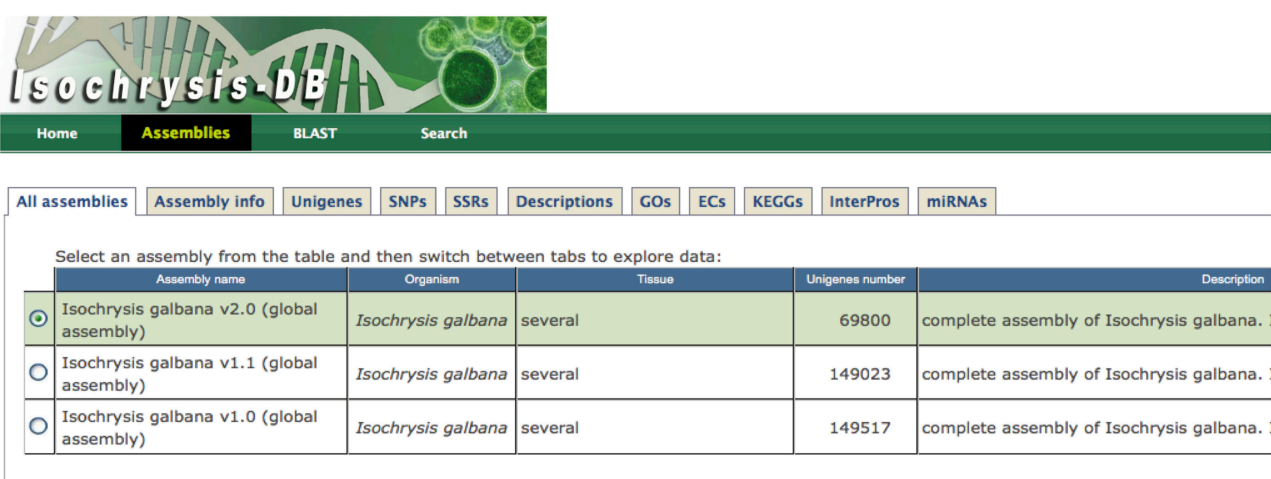
## Expression Patterns During Microalgal Growth

Growth of *T. lutea* under controlled conditions of temperature and illumination was monitored for 17 days and cell density was estimated daily. The exponential phase lasted until the day 6, the phase of declining relative growth from days 6 to 9, the stationary phase from days 9 to 15 and the death phase from days 15 to 17 (Figure 3, left upper panel). Expression profiles indicated a significant increase of mRNA levels for *perox*, *apx3*, *ahp1*, *sod2*, *aryl*, and *dio* transcripts along the growth curve (Figures 3, 4). A wide set of transcripts (including *aryl*, *ccp*, *perox*, *sod1*, *sod2*, *sod3*, *apx3*, *ahp1*, and *dio*) peaked their mRNA levels coinciding with declining growth rate and the beginning of stationary phase, with small gene-specific differences in the peaking time (Figures 3, 4). Thereafter, most of these transcripts reduced expression except *ahp1* and *dio*, which increased their expression at the end of the stationary phase. Unlike these transcripts, the *gpx1* transcript decreased its expression progressively during the growth of *T. lutea*, and no significant differences were observed in *apx2* and *ahp2* mRNA levels (Figures 3, 4).

## Effects of Iodide and Iodate on Gene Expression

In order to determine the effects of iodide and iodate on gene expression, mRNA levels of selected transcripts were quantified in *T. lutea* cultures exposed to 5 mM iodide and 5 mM iodate for 3 h. Iodide significantly up-regulated *perox* gene expression (2.25-fold with respect to the untreated control). In contrast,

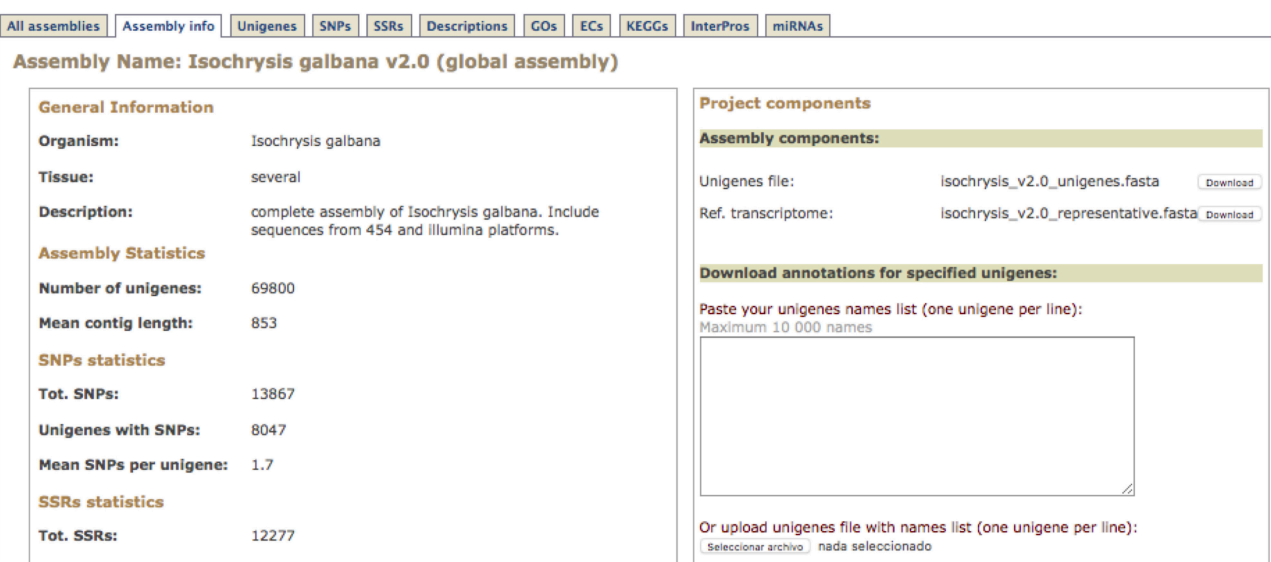
**A**



Select an assembly from the table and then switch between tabs to explore data:

| Assembly name  | Organism                  | Tissue  | Unigenes number | Description                                      |
|--|---------------------------|---------|-----------------|--|
| <input checked="" type="radio"/> Isochrysis galbana v2.0 (global assembly) | <i>Isochrysis galbana</i> | several | 69800           | complete assembly of <i>Isochrysis galbana</i> . |
| <input type="radio"/> Isochrysis galbana v1.1 (global assembly)            | <i>Isochrysis galbana</i> | several | 149023          | complete assembly of <i>Isochrysis galbana</i> . |
| <input type="radio"/> Isochrysis galbana v1.0 (global assembly)            | <i>Isochrysis galbana</i> | several | 149517          | complete assembly of <i>Isochrysis galbana</i> . |

**B**



**Assembly Name: *Isochrysis galbana* v2.0 (global assembly)**

**General Information**

**Organism:** *Isochrysis galbana*

**Tissue:** several

**Description:** complete assembly of *Isochrysis galbana*. Include sequences from 454 and Illumina platforms.

**Assembly Statistics**

**Number of unigenes:** 69800

**Mean contig length:** 853

**SNPs statistics**

**Tot. SNPs:** 13867

**Unigenes with SNPs:** 8047

**Mean SNPs per unigene:** 1.7

**SSRs statistics**

**Tot. SSRs:** 12277

**Project components**

**Assembly components:**

Unigenes file: [isochrysis\\_v2.0\\_unigenes.fasta](#)

Ref. transcriptome: [isochrysis\\_v2.0\\_representative.fasta](#)

**Download annotations for specified unigenes:**

Paste your unigenes names list (one unigene per line):  
Maximum 10 000 names

Or upload unigenes file with names list (one unigene per line):  
 nada seleccionado

**FIGURE 1** | IsochrysisDB interface. **(A)** “Assemblies” tab containing all information about transcriptomes; **(B)** Navigation window for *T. lutea* v2.0 that includes the different tabs (“Assembly info,” “Unigenes,” “SNPs,” “SSRs,” “Descriptions,” “GO,” “ECs,” “KEGGs,” “InterPros,” and “miRNAs”) is shown. Moreover, the fasta files for full and reference transcriptomes are available in the assembly components section.

iodate increased *gpx1* mRNA levels (3.12-fold) and down-regulated *ccp* gene expression (1.96-fold) (Table 4). A further analysis of activated genes (*perox* and *gpx1*) 6 h after the treatment confirmed the expression profiles (Figure S2).

## Effects of H<sub>2</sub>O<sub>2</sub> and Iodide on Gene Expression

In order to evaluate a possible interaction between iodide levels and H<sub>2</sub>O<sub>2</sub> to modulate gene expression, a preliminary trial was carried out to evaluate the removal rate of H<sub>2</sub>O<sub>2</sub> either in the presence or absence of iodide using ASW and *T. lutea* cells. In ASW free of *T. lutea* cells and without any added iodide, the

H<sub>2</sub>O<sub>2</sub> reduction was ~7% of initial H<sub>2</sub>O<sub>2</sub> concentration after 6 h. The addition of iodide to the ASW clearly accelerated the removal of H<sub>2</sub>O<sub>2</sub> ( $p < 0.01$ ; Figure 5). On the other hand, when H<sub>2</sub>O<sub>2</sub> was added to the microalgae cultures, 90% was rapidly removed in 45 min independently of iodide levels. Following these results, a new trial using microalgae in exponential phase and exposed to both H<sub>2</sub>O<sub>2</sub> and iodide was carried out and gene expression of a subset of genes involved in oxidative stress and iodide regulation quantified at 5 and 45 min after treatments.

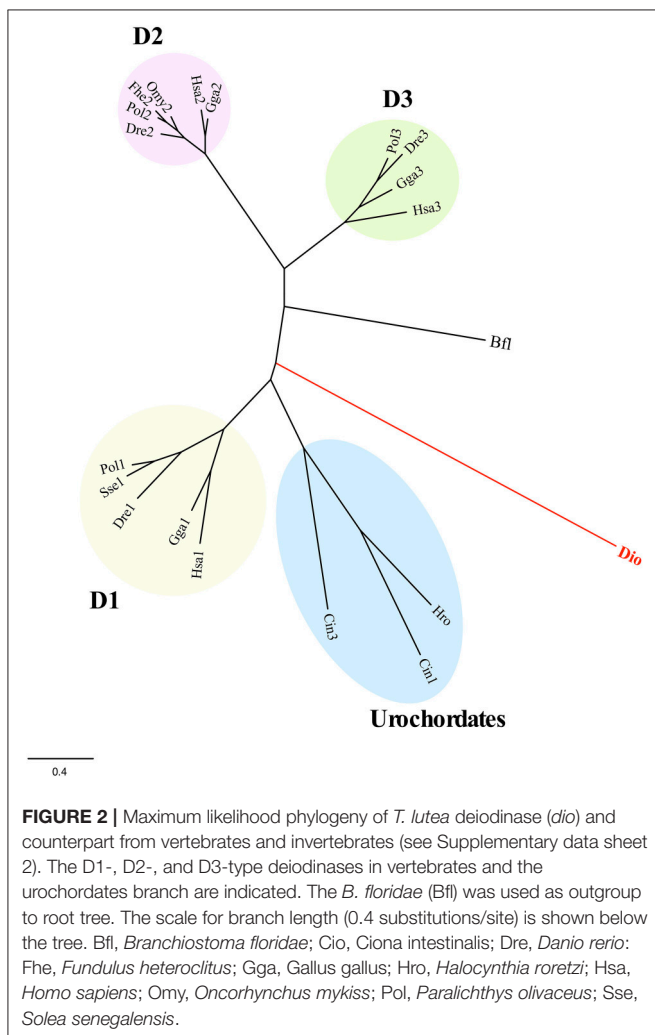
H<sub>2</sub>O<sub>2</sub> treatments significantly activated the expression of *perox*, *gpx1*, *apx2*, *apx3*, *ahp1*, *ahp2*, *sod1*, *sod3*, and *aryl* ( $p < 0.05$ ) although with temporal differences, confirming their



**TABLE 3** | Homologous sequences to transcripts selected for PCR studies.

| Transcript   | Homologous                            | N°  | Conserved domain/annotation (best hit)      | Taxa   |
|--------------|---------------------------------------|-----|---|--|
| <i>ccp</i>   | Eukaryota                             | 100 | Plant peroxidase superfamily                | Protist/Fungi  |
| <i>gpx1</i>  | Eukaryota                             | 95  | Thioredoxin superfamily                     | Protist/Plantae/Vertebrates/Arthropoda/Mollusks                |
| <i>perox</i> | Stylonychia lemame                    | 6   | Arachidonate 12–12 s                        | Ciliate  |
|              | Oxytricha trifallax                   | 7   | Putative peroxidase                         | Ciliate  |
|              | Acanthamoeba castellanii str. Neff    | 3   | Animal heme peroxidase                      | Amoeba   |
|              | Pseudobacteriovorax antillogorgiicola | 1   | Hypothetical protein                        | Bacteria   |
|              | Symbiodinium microadriaticum          | 1   | NAD-dependent protein deacetylase sirtuin-2 | Dinoflagellates  |
| <i>apx2</i>  | Eukaryota                             | 100 | Plant peroxidase superfamily                | Protist/Plantae/Fungi  |
| <i>apx3</i>  | Eukaryota                             | 100 | Plant peroxidase superfamily                | Protist/Plantae/Fungi  |
| <i>sod1</i>  | Bacteria                              | 86  | No domain/Superoxide dismutase              | Gram +/G-proteobacteria  |
| <i>sod2</i>  | Bacteria                              | 100 | No domain/Superoxide dismutase              | Gram +   |
| <i>sod3</i>  | Eukaryota/Bacteria                    | 100 | Sod_Fe_C superfamily (SodA)                 | Protist/Plantae/Cyanobacteria/Firmicutes/Sphingobacteria       |
| <i>aryl</i>  | Eukaryota/Bacteria                    | 83  | Alpha/beta-hydrolase superfamily            | Protist  |
| <i>ahp1</i>  | Eukaryota/Bacteria                    | 99  | Thioredoxin superfamily                     | Proteobacteria/Enterobacteria/Cyanobacteria/Firmicutes/Protist |
| <i>ahp2</i>  | Bacteria                              | 79  | Thioredoxin superfamily                     | Firmicutes/Proteobacteria/Sphingobacteria                      |
| <i>dio</i>   | Bilateria                             | 89  | Thioredoxin superfamily                     | Vertebrates  |

BLASTx searches using the transcripts as seed in NCBI database.

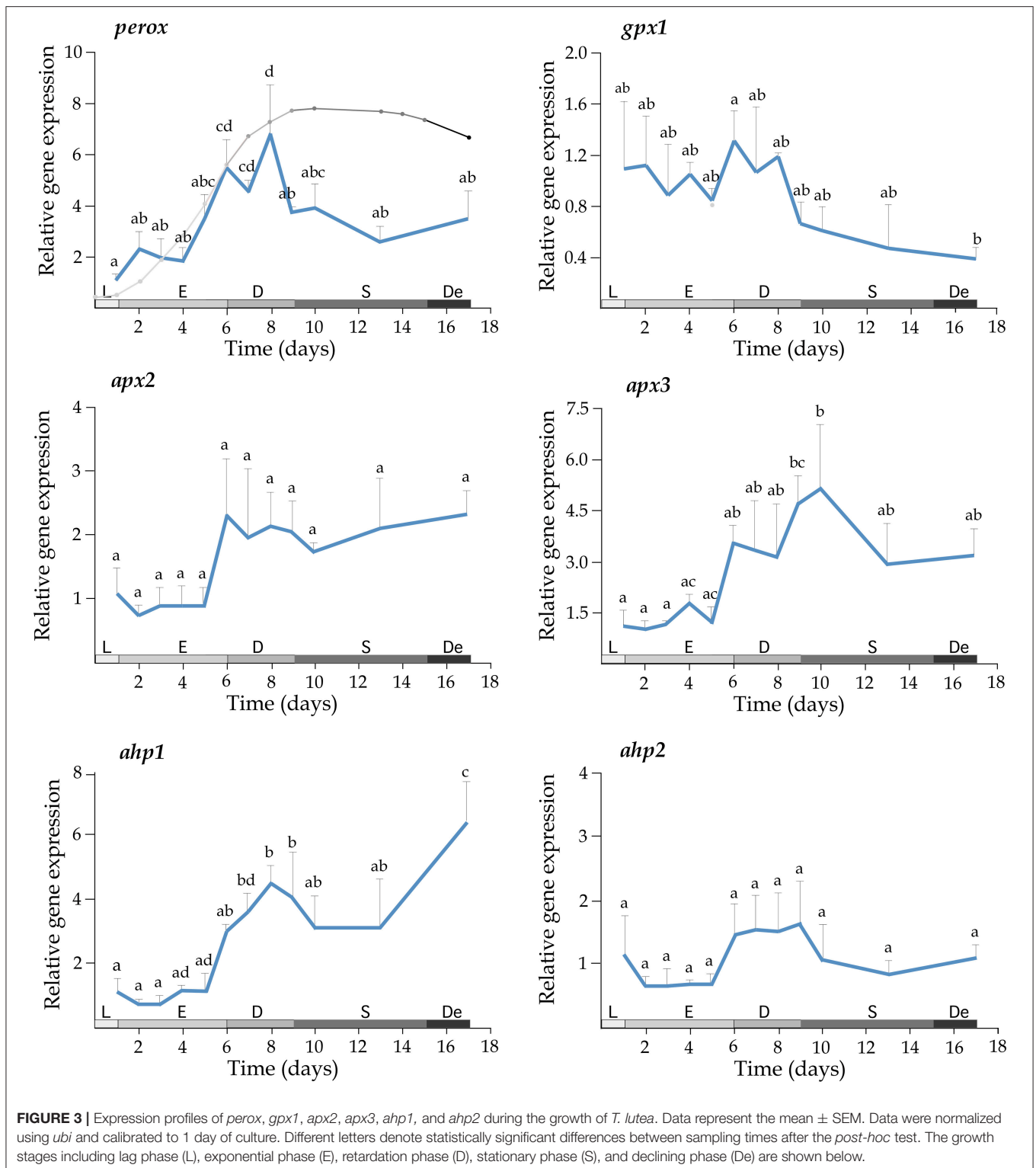


participation in antioxidant defensive response to detoxify  $H_2O_2$  (Figures 6 and Figure S3). However, only *apx2* and *perox* showed a significant response to iodide treatments. The *apx2* mRNA levels were lower in the iodide-treated samples but the activation response to  $H_2O_2$  was not dependent on iodide levels. On the contrary, mRNA *perox* abundance was higher in iodide treated cells. More interestingly, the transcriptional induction triggered by  $H_2O_2$  in this gene was highly dependent on the presence of iodide to the medium. This observation was consistent in a different experimental replicate in which iodide treatments were done during separate experiments (Figure S3).

## DISCUSSION

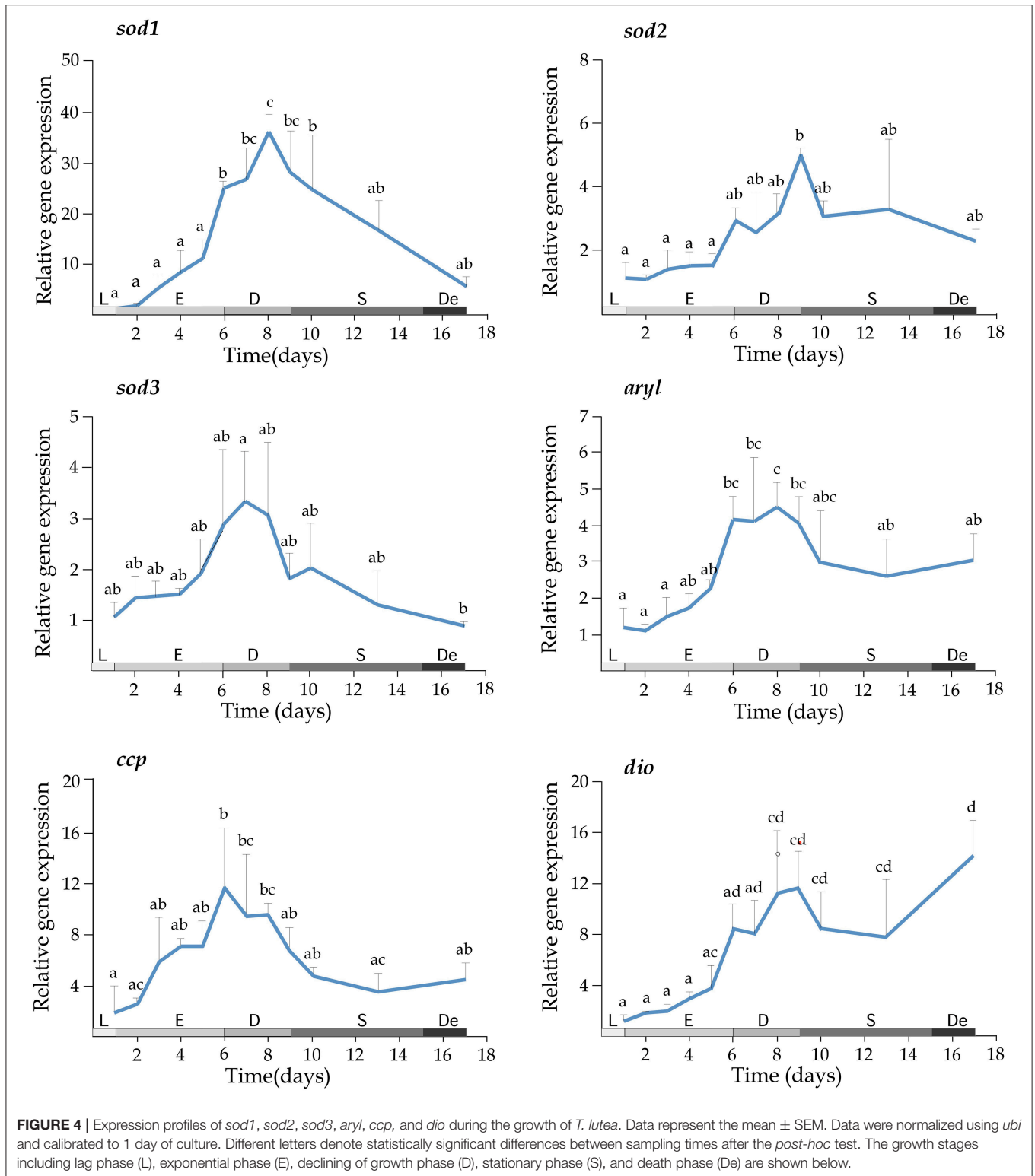
The metabolism of iodine in microalgae is far to be properly understood. In this study, the transcriptome of *T. lutea*, one microalga that accumulates THs, using both long (Roche/454) and short (Illumina) reads was assembled. A previous transcriptome of *T. lutea* using cells in the retardation phase cultivated standard culture conditions in batch was reported (Carrier et al., 2014), however, our experimental conditions using cells in exponential phase cultivated under high iodide and peroxide treatments enriched in transcripts specifically related with iodine metabolism. Although normalized libraries were originally intended to minimize transcript redundancy, the cleaning results indicated a high number of rejected sequences, most of them from plastids (66.2% in 454 and 68.3% in Illumina). These data agree with previous data from our group in the flatfish *Solea senegalensis*, in which 454-normalized libraries resulted in a high rate of rejected redundant sequences and more fragmented assemblies (Benzekri et al., 2014). Our data confirm that normalization is not a good strategy when a maximal number of correctly predicted full-length cDNAs is intended unless a deep coverage is expected (Cahais et al., 2012).





The full transcriptome *T. lutea*v2 contained 69,800 valid transcripts that resulted in a reference transcriptome of 23,671 transcripts with similar GO categories representation. This reference transcriptome is considered a useful tool for deep sequencing studies to minimize data processing times

without losing any significant information about regulatory pathways in the functional analysis (Hachero-Cruzado et al., 2014; Fatsini et al., 2016). Sequence comparisons of the reference transcriptome with the previously published transcriptome in *T. lutea* (Carrier et al., 2014) indicated an



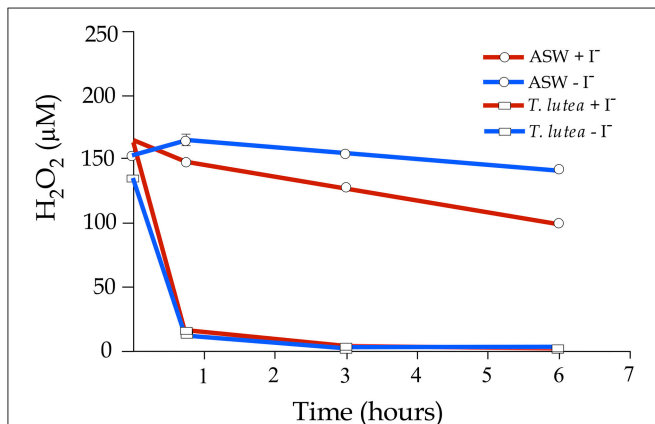
almost complete matching (98.7%). Nevertheless, comparison of full transcriptomes reduced similarities between 89.3 and 92.0% indicating a small subset of assembly-specific transcripts that could be due to different experimental conditions, strains

or assembly artifacts. In any case, both transcriptomes represent a valuable genomic information for the annotation and characterization of the upcoming genome of this microalga of high importance in aquaculture and biotechnology.

**TABLE 4** | Expression levels of *perox*, *gpx1*, *apx2*, *apx3*, *sod1*, *sod2*, *sod3*, *aryl*, *ccp*, and *dio* in *T. lutea* cultures at 3 h after iodide (5 mM) or iodate (5 mM).

| Transcript name | Control                  | Iodide                   | Iodate                   |
|-----------------|--------------------------|--------------------------|--------------------------|
| <i>perox</i>    | 1.18 ± 0.15 <sup>a</sup> | 2.25 ± 0.38 <sup>b</sup> | 1.58 ± 0.32 <sup>a</sup> |
| <i>gpx1</i>     | 1.09 ± 0.52 <sup>a</sup> | 0.98 ± 0.28 <sup>a</sup> | 3.12 ± 0.44 <sup>b</sup> |
| <i>apx2</i>     | 1.07 ± 0.45              | 0.95 ± 0.10              | 1.03 ± 0.03              |
| <i>apx3</i>     | 1.01 ± 0.16              | 1.10 ± 0.46              | 0.70 ± 0.19              |
| <i>sod1</i>     | 1.00 ± 0.12              | 1.20 ± 0.24              | 1.17 ± 0.39              |
| <i>sod2</i>     | 1.01 ± 0.16              | 1.14 ± 0.15              | 0.81 ± 0.24              |
| <i>sod3</i>     | 1.01 ± 0.17              | 0.72 ± 0.25              | 0.83 ± 0.09              |
| <i>aryl</i>     | 1.01 ± 0.16              | 1.06 ± 0.13              | 0.95 ± 0.12              |
| <i>ccp</i>      | 1.01 ± 0.14 <sup>a</sup> | 0.94 ± 0.29 <sup>a</sup> | 0.51 ± 0.11 <sup>b</sup> |
| <i>dio</i>      | 1.02 ± 0.12              | 1.10 ± 0.22              | 1.23 ± 0.23              |

An untreated control, without addition of any chemical, was also done. Expression data are calibrated to the untreated control and expressed as mean ± SEM ( $n = 3$ ). The letters denote statistically significant differences among treatments after the post-hoc analysis.

**FIGURE 5** | Hydrogen peroxide decomposition in artificial seawater (ASW) and in an exponential culture of *T. lutea*. Half of the samples were added iodide (500 μM) and then all samples were treated with H<sub>2</sub>O<sub>2</sub> (200 μM). H<sub>2</sub>O<sub>2</sub> levels were monitored for 6 h. Bars represent mean values ± SEM ( $n = 4$ ). Red lines indicated iodide-added samples and blue lines the controls without iodide.

It is noteworthy that all transcriptomes assembled in this study were hosted in a specific database named IsochrysisDB. The information was structured in a similar way to SoleaDB (Benzekri et al., 2014), EuroPineDB (Fernández-Pozo et al., 2011), EuroPineDB (Fernández-Pozo et al., 2011), and ReprOlive (Carmona et al., 2015). All transcriptomic information can be browsed by assemblies (with history versions) that contains all relevant information about bioinformatic pipeline, experimental conditions and main statistical features. Within each assembly, all information about the transcript sequences, ORF prediction, annotations (including GO, KEGGs, InterPros) and molecular markers (SNPs and SSRs) can be browsed. Moreover, custom searches by keywords and Blast can be carried out to rapidly identify target sequences. This database represents a powerful tool for research focused on microalgae genomics, specifically in *T. lutea* that can be progressively updated to improve the current information and provide new services for transcriptomics.

Our experimental design used a permanent and non-saturating illumination conditions that ensured stable oxidative stress conditions. The irradiance used was well below photoinhibition values as demonstrated by optimal quantum yield achieved (van Bergeijk et al., 2016). Under these conditions, a set of transcripts related to iodine and/or oxidative metabolism were identified in the IsochrysisDB and were further characterized by *in silico* and gene expression analyses. Of particular interest are the peroxidases since they play a central role in H<sub>2</sub>O<sub>2</sub> detoxification and iodine uptake and organification. All peroxidases showed a high number of homologous sequences in other microalgae and bacteria except *perox* that had low identities with respect to protist homologs (ciliates and amoeboids). The best hit indicated that the closest peroxidase is in *Acanthanieba castellanii* homolog, an animal-like heme-dependent peroxidase (Clarke et al., 2013), that belongs to the peroxidase-cyclooxygenase family, which includes among others the myeloperoxidase or thyroid peroxidase (Zámocký and Obinger, 2010; Zámocký et al., 2014). We hypothesize that *T. lutea* could have retained this peroxidase by HGT. Extensive bacterium-derived HGT not related to plastid functions has been described in red algal genomes (Qiu et al., 2013, 2015). More importantly, these non-endosymbiont gene transfers can be propagated through additional rounds of secondary and tertiary endosymbiosis to several other protist hosts such as stramenopiles, alveolates, haptophytes, cryptophytes, and amoeba (Qiu et al., 2013), supporting the HGT as the most plausible hypothesis with fixation in some specific protist lineages.

A striking result was the identification of a type I iodothyronine deiodinase-like sequence in *T. lutea*. In vertebrates, this kind of enzyme plays a key role in the peripheral regulation of THs actions catalyzing the conversion of T<sub>4</sub> to the active form T<sub>3</sub> (Alves et al., 2017). Although the thyroid system appeared at the beginning of vertebrate evolution, some studies reported thyroxine deiodinases in invertebrates and social amoebas (Heyland et al., 2006; Lobanov et al., 2007; Wu et al., 2012; Singh et al., 2014). Our study is the first report identifying a thyroxine deiodinase in a microalga species with capacity to synthesize TH-like compounds (Heyland and Moroz, 2005) representing one of the most ancestral deiodinase that later propagated in eukaryote lineages. The molecular analysis identified a Cys instead of SeCys in the active site as occurs in some dictyostelids and the cephalochordate amphioxus *Branchiostoma floridae* (Holland et al., 2008; Klootwijk et al., 2011; Singh et al., 2014) indicating that ancestral deiodinases lacked the selenocysteine. The residue in the active site not only modulates catalytic efficiency but also molecule affinity as observed *B. floridae* biasing preferentially the activity toward the 3,3',5'-triiodothyroacetic acid (TA<sub>3</sub>) and tetraiodothyroacetic acid (TA<sub>4</sub>) instead of triiodothyronine (T<sub>3</sub>) and tetraiodothyronine (T<sub>4</sub>) (Paris et al., 2008). Some authors have suggested the TA<sub>3</sub> as the ancient bioactive hormone whereas T<sub>3</sub> acquired a predominant role later during evolution probably reflecting a co-evolution enzyme and substrate (Klootwijk et al., 2011). In any case, the identification of TH-like compounds in some microalgae including *T. lutea* (Heyland and Moroz,

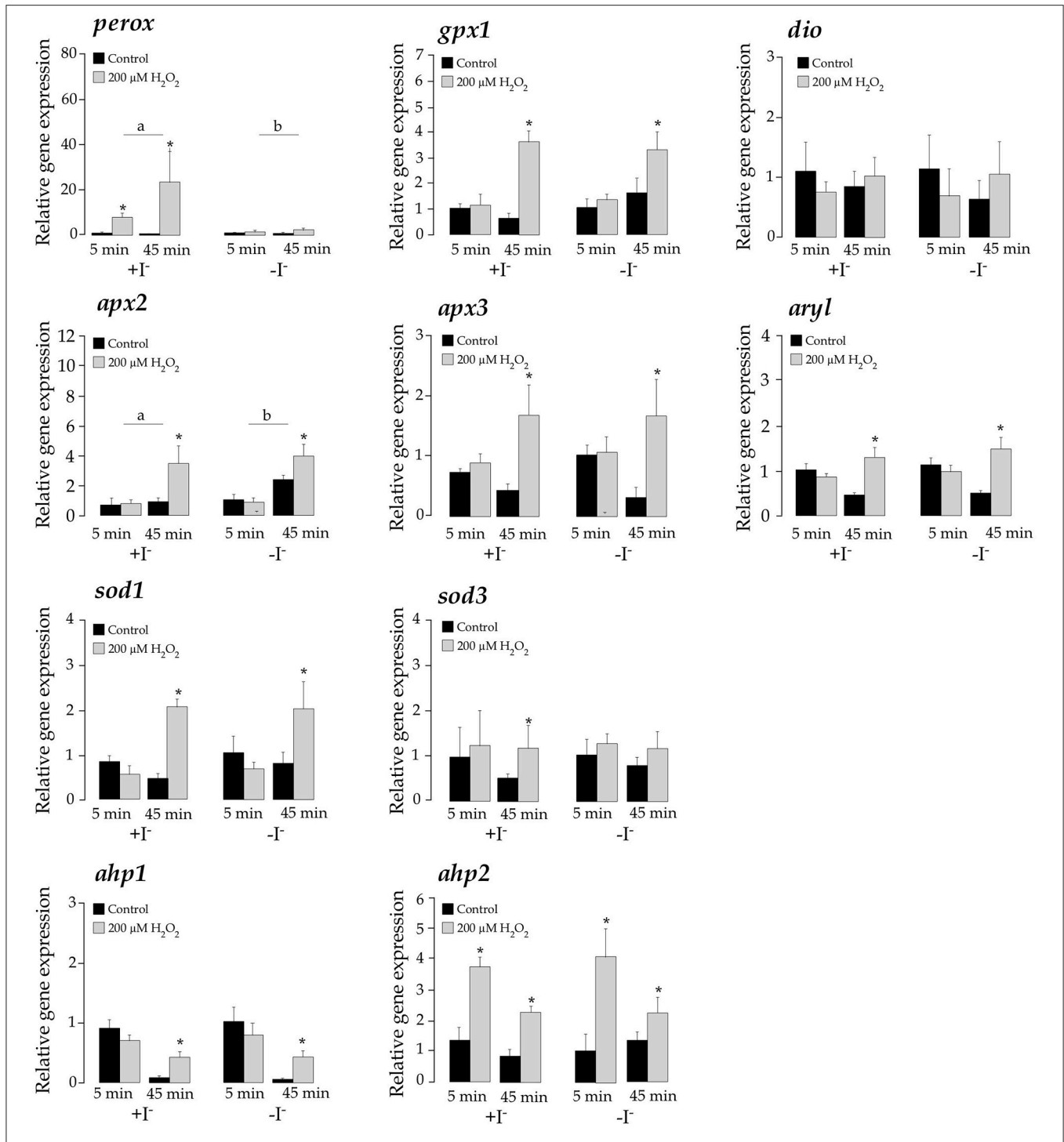


**FIGURE 6** | Expression levels of *perox*, *gpx1*, *dio*, *apx2*, *apx3*, *aryl*, *sod1*, *sod3*, *ahp1*, and *ahp2* in *T. lutea* cultures at 5 and 45 min after adding iodide (+I<sup>-</sup>) or not (-I<sup>-</sup>) followed by a H<sub>2</sub>O<sub>2</sub> treatment (200 μM). Negative controls without H<sub>2</sub>O<sub>2</sub> treatments were also done for each iodide concentration. Data represent the mean ± SEM. The asterisk denotes statistically significant differences between non-treated and H<sub>2</sub>O<sub>2</sub>-treated at each sampling point and iodide condition. The letters denote significant differences between iodide-added and non-iodide added samples. All data were calibrated to the 5 min control samples added iodide without H<sub>2</sub>O<sub>2</sub>.

2005) suggests that this novel deiodinase should participate in TH metabolism. The increase of *dio* mRNA levels during the exponential growth phase, in a similar way to most

antioxidant genes, suggests this enzyme acts modulating the bulk of intracellular iodide to scavenge ROS (Venturi, 2011). It is thus likely that iodide mobilization might contribute to



the pool of antioxidant mechanisms acting in response to elevated ROS production due to high photosynthetic activity during exponential growth. The nature of the response of marine microalgae to irradiance is highly species-specific (Janknegt et al., 2009) and iodide could be playing a yet uncovered function at this regard. The later increase of *dio* in the declining phase suggests an additional role for iodide in other cellular processes not directly linked to photosynthesis. In mammals, molecular iodine induces cell death through the activation of a mitochondria-mediated apoptotic pathway (Shrivastava et al., 2006) and in the amoeba *D. discoideum*, the deiodinase is essential for the formation of multiple signaling centers regulating growth and development (Singh et al., 2014) indicating that deiodinase could also regulate gene life cycle in the microalga.

In batch-cultures, the stationary growth phase coincides with a decrease in cell viability, depletion of pigments and essential nutrients and deterioration of thylakoid membranes. Under these conditions, photosynthetic rates and CO<sub>2</sub> fixation drop resulting in different metabolic processes becoming more relevant at generating oxidative stress (Sigaud-Kutner et al., 2002, 2005; Liu et al., 2012). Cells then need to rearrange mobilization of oxidative defense mechanisms including peroxidases, SODs, and other antioxidant defenses such as carotenoids (Blokina et al., 2003). Although previous studies in diverse microalgae demonstrated absence of correlation between irradiance intensity and SOD activity (Janknegt et al., 2009), an increased SOD activity in the stationary growth phase associated to oxidative stress has been reported (Sigaud-Kutner et al., 2002). Moreover, SOD, catalase and APx activities are also activated under nitrogen depletion to cope with the physiological stress induced by such condition (Yilancioglu et al., 2014). In this study, we demonstrated a coordinated activation of genes involved in ROS detoxification, including SOD (*sod1*, *sod2*, *sod3*) and peroxidases (*apx3*, *aryl*, *ccp*, *perox*, *ahp1*) that peaked at the beginning of the stationary phase, when nutrients started to be depleted (Liu et al., 2012) indicating that cells activated antioxidant enzymes transcripts coinciding with ROS production likely derived from nutrient scarcity.

External addition of H<sub>2</sub>O<sub>2</sub> rapidly activated the expression of some peroxidases (*perox*, *gpx1*, *apx2*, *apx3*, *aryl*) and even of two SODs (*sod1* and *sod3*) to quickly remove toxic levels from the *T. lutea* cultures (Figure 6). The *perox* and *ahp2* rapidly expressed after 5 min of the H<sub>2</sub>O<sub>2</sub> insult, whereas *gpx1*, *sod1*, *sod3*, *apx2*, *apx3*, *aryl*, and *ahp1* increased later, after 45 min. These temporal expression patterns might be associated with the nature of the detoxifying activity and its localization in the cell. The activation of SOD-encoding genes by H<sub>2</sub>O<sub>2</sub> could be an indirect effect resulting of a change cell redox state that can activate a global defensive response in the cell. A similar effect was detected in *E. coli* in which an external H<sub>2</sub>O<sub>2</sub> insult could activate the regulator SoxRS and trigger the expression of several genes related with detoxification of O<sub>2</sub><sup>•−</sup> (Manchado et al., 2000). However, the most striking result is the iodide-dependent response of *perox* gene expression after the H<sub>2</sub>O<sub>2</sub> treatment. A search in the IsochrysisDB by annotations or blast failed to identify any haloperoxidase-encoding sequence in *T. lutea*. However, the dependence of *perox* expression on environmental iodide (and

not iodate), as revealed by threshold mRNA abundance and the response to H<sub>2</sub>O<sub>2</sub>, indicates that this gene could be a putative haloperoxidase. A previous study of our group indicated that iodide uptake in *T. lutea* could possibly be promoted by an enzymatic oxidation using H<sub>2</sub>O<sub>2</sub> (van Bergeijk et al., 2013). The similarity of *perox* with peroxidase-cyclooxygenases in metazoans and its origin by HGT, as previously discussed, makes this gene a good candidate to participate in iodide metabolism processes such as uptake and organification and it could thus also have an impact on the biosynthesis of TH-like-compounds. Further studies will be necessary to elucidate the precise role of this enzyme on THs metabolism in *T. lutea*.

In conclusion, the transcriptomic analysis and the database IsochrysisDB provided new genomic resources to boost research in *T. lutea* improving the management of information and our understanding about the molecular mechanisms that control iodide and oxidative metabolism in microalgae. Moreover, some genes involved in ROS detoxification were identified and characterized. Of particular interest is the identification of one iodothyronine deiodinase and one putative haloperoxidase that could represent the ancestral origin of TH-signaling and hence be essential to understand the evolution of TH in vertebrates.

## AUTHOR CONTRIBUTIONS

JC, MM, and SvB conceived the overall study. LH and SvB carried out the microalgae trials and sample preparation. MM carried out the qPCR analyses and wrote the manuscript with contributions from all coauthors. HB and MC carried out the bioinformatic analysis (assembly, annotation and database development). MG prepared RNA-seq libraries and sequenced iodide- and peroxide-treated samples.

## ACKNOWLEDGMENTS

This study was carried out in the framework of research project RTA2009-00054-00-00, funded by the Instituto Nacional de Investigación y Tecnología Agraria y Alimentaria (INIA) and European Regional Development Funds and the FEDER project Nuevas herramientas genómicas para el análisis genético y evaluación transcriptómica de compuestos funcionales basados en microalgas para impulsar la acuicultura del lenguaje (SOLEALGAE) PP.AVA.AVA201601.9 cofunded 80% by Fondo Europeo de Desarrollo Regional, dentro del Programa Operativo FEDER de Andalucía 2014-2020. We wish to thank to Dr. Miguel Ángel Cevallos and Dr. Santiago Castillo Ramírez from Center for Genomic Sciences at Mexico for their comments and support during the preparation of this manuscript. Additionally, LH is thankful to the Center for Genomic Sciences and the Mexican Secretary of Foreign Affairs, which supported her by a fellowship (AMEXCID number HERLAU8104116) during the preparation of this manuscript.

## SUPPLEMENTARY MATERIAL

The Supplementary Material for this article can be found online at: <https://www.frontiersin.org/articles/10.3389/fmars.2018.00134/full#supplementary-material>

## REFERENCES

- Alves, R. N., Cardoso, J. C., Harboe, T., Martins, R. S., Machado, M., Norberg, B., et al. (2017). Duplication of Dio3 genes in teleost fish and their divergent expression in skin during flatfish metamorphosis. *Gen. Comp. Endocrinol.* 246, 279–293. doi: 10.1016/j.ygcen.2017.01.002
- Bendif, E. M., Probert, I., Schroeder, D. C., and De Vargas, C. (2013). On the description of *Tisochrysis lutea* gen. nov. sp. nov. and *Isochrysis nuda* sp. nov. in the Isochrysidales, and the transfer of Dicrateria to the Prymnesiales (Haptophyta). *J. Appl. Phycol.* 25, 1763–1776. doi: 10.1007/s10811-013-0037-0
- Benzekri, H., Armesto, P., Cousin, X., Rovira, M., Crespo, D., Merlo, M. A., et al. (2014). *De novo* assembly, characterization and functional annotation of Senegalese sole (*Solea senegalensis*) and common sole (*Solea solea*) transcriptomes: integration in a database and design of a microarray. *BMC Genomics* 15:952. doi: 10.1186/1471-2164-15-952
- Blokhina, O., Virolainen, E., and Fagerstedt, K. V. (2003). Antioxidants, oxidative damage and oxygen deprivation stress: a review. *Ann. Bot.* 91, 179–194. doi: 10.1093/aob/mcf118
- Cahais, V., Gayral, P., Tsagkogeorga, G., Melo-Ferreira, J., Ballenghien, M., Weinert, L., et al. (2012). Reference-free transcriptome assembly in non-model animals from next-generation sequencing data. *Mol. Ecol. Resour.* 12, 834–845. doi: 10.1111/j.1755-0998.2012.03148.x
- Carmona, R., Zafra, A., Seoane, P., Castro, A. J., Guerrero-Fernandez, D., Castillo-Castillo, T., et al. (2015). ReprOlive: a database with linked data for the olive tree (*Olea europaea* L.) reproductive transcriptome. *Front. Plant Sci.* 6:625. doi: 10.3389/fpls.2015.00625
- Carrier, G., Garnier, M., Le Cunff, L., Bougaran, G., Probert, I., De Vargas, C., et al. (2014). Comparative transcriptome of wild type and selected strains of the microalgae *Tisochrysis lutea* provides insights into the genetic basis, lipid metabolism and the life cycle. *PLoS ONE* 9:e86889. doi: 10.1371/journal.pone.0086889
- Chapman, R. L. (2013). Algae: the world's most important “plants”—an introduction. *Mitig. Adapt. Strateg. Glob. Change* 18, 5–12. doi: 10.1007/s11027-010-9255-9
- Chevreau, B., Pfisterer, T., Drescher, B., Driesel, A. J., Muller, W. E., Wetter, T., et al. (2004). Using the miraEST assembler for reliable and automated mRNA transcript assembly and SNP detection in sequenced ESTs. *Genome Res.* 14, 1147–1159. doi: 10.1101/gr.1917404
- Chino, Y., Saito, M., Yamasu, K., Suyemitsu, T., and Ishihara, K. (1994). Formation of the adult rudiment of sea urchins is influenced by thyroid hormones. *Dev. Biol.* 161, 1–11. doi: 10.1006/dbio.1994.1001
- Cirulis, J. T., Scott, J. A., and Ross, G. M. (2013). Management of oxidative stress by microalgae. *Can. J. Physiol. Pharmacol.* 91, 15–21. doi: 10.1139/cjpp-2012-0249
- Clarke, M., Lohan, A. J., Liu, B., Lagkouvardos, I., Roy, S., Zafar, N., et al. (2013). Genome of *Acanthamoeba castellanii* highlights extensive lateral gene transfer and early evolution of tyrosine kinase signaling. *Genome Biol.* 14:R11. doi: 10.1186/gb-2013-14-2-r11
- Colin, C., Leblanc, C., Michel, G., Wagner, E., Leize-Wagner, E., Van Dorsselaer, A., et al. (2005). Vanadium-dependent iodoperoxidases in *Laminaria digitata*, a novel biochemical function diverging from brown algal bromoperoxidases. *J. Biol. Inorg. Chem.* 10, 156–166. doi: 10.1007/s00775-005-0626-8
- Crockford, S. J. (2009). Evolutionary roots of iodine and thyroid hormones in cell-cell signaling. *Integr. Comp. Biol.* 49, 155–166. doi: 10.1093/icb/icip053
- Falgueras, J., Lara, A. J., Fernandez-Pozo, N., Canton, F. R., Perez-Trabado, G., and Claros, M. G. (2010). SeqTrim: a high-throughput pipeline for pre-processing any type of sequence read. *BMC Bioinformatics* 11:38. doi: 10.1186/1471-2105-11-38
- Falkowski, P. (2012). Ocean science: the power of plankton. *Nature* 483, S17–S20. doi: 10.1038/483S17a
- Fatsini, E., Bautista, R., Machado, M., and Duncan, N. J. (2016). Transcriptomic profiles of the upper olfactory rosette in cultured and wild Senegalese sole (*Solea senegalensis*) males. *Comp. Biochem. Physiol. Part D Genomics Proteomics* 20, 125–135. doi: 10.1016/j.cbd.2016.09.001
- Fernández-Pozo, N., Canales, J., Guerrero-Fernandez, D., Villalobos, D. P., Diaz-Moreno, S. M., Bautista, R., et al. (2011). EuroPineDB: a high-coverage web database for maritime pine transcriptome. *BMC Genomics* 12:366. doi: 10.1186/1471-2164-12-366
- Gribble, G. W. (2003). The diversity of naturally produced organohalogenes. *Chemosphere* 52, 289–297. doi: 10.1016/S0045-6535(03)00207-8
- Gribble, G. W. (2015). Biological activity of recently discovered halogenated marine natural products. *Mar. Drugs* 13, 4044–4136. doi: 10.3390/md13074044
- Guedes, A. C., and Malcata, F. X. (2012). “Nutritional value and uses of microalgae in aquaculture,” in *Aquaculture*, ed Z. Muchlisin (Rijeka: InTech), 59–78.
- Gwon, H. J., Teruhiko, I., Shigeaki, H., and Baik, S. H. (2014). Identification of novel non-metal haloperoxidases from the marine metagenome. *J. Microbiol. Biotechnol.* 24, 835–842. doi: 10.4014/jmb.1310.10070
- Hachero-Cruzado, I., Rodriguez-Rua, A., Roman-Padilla, J., Ponce, M., Fernandez-Diaz, C., and Machado, M. (2014). Characterization of the genomic responses in early Senegalese sole larvae fed diets with different dietary triacylglycerol and total lipids levels. *Comp. Biochem. Physiol. Part D Genomics Proteomics* 12, 61–73. doi: 10.1016/j.cbd.2014.09.005
- Heyland, A., and Moroz, L. L. (2005). Cross-kingdom hormonal signaling: an insight from thyroid hormone functions in marine larvae. *J. Exp. Biol.* 208, 4355–4361. doi: 10.1242/jeb.01877
- Heyland, A., Price, D. A., Bodnarova-Buganova, M., and Moroz, L. L. (2006). Thyroid hormone metabolism and peroxidase function in two non-chordate animals. *J. Exp. Zool. B Mol. Dev. Evol.* 306, 551–566. doi: 10.1002/jez.b.21113
- Hill, V., and Manley, S. (2009). Release of reactive bromine and iodine from diatoms and its possible role in halogen transfer in polar and tropical oceans. *Limnol. Oceanogr.* 54, 812–822. doi: 10.4319/lo.2009.54.3.0812
- Holland, L. Z., Albalat, R., Azumi, K., Benito-Gutierrez, E., Blow, M. J., Bronner-Fraser, M., et al. (2008). The amphioxus genome illuminates vertebrate origins and cephalochordate biology. *Genome Res.* 18, 1100–1111. doi: 10.1101/gr.073676.107
- Hughes, C., and Sun, S. (2016). Light and brominating activity in two species of marine diatom. *Mar. Chem.* 181, 1–9. doi: 10.1016/j.marchem.2016.02.003
- Iwamoto, K., and Shiraiwa, Y. (2012). Characterization of intracellular iodine accumulation by iodine-tolerant microalgae. *Proced. Environ. Sci.* 15, 34–42. doi: 10.1016/j.proenv.2012.05.007
- Janknegt, P. J., De Graaff, C. M., Van De Poll, W. H., Visser, R. J. W., Rijstenbil, J. W., and Buma, A. G. J. (2009). Short-term antioxidative responses of 15 microalgae exposed to excessive irradiance including ultraviolet radiation. *Eur. J. Phycol.* 44, 525. doi: 10.1080/09670260902943273
- Klootwijk, W., Friesema, E. C., and Visser, T. J. (2011). A nonselenoprotein from amphioxus deiodinates triac but not T3: is triac the primordial bioactive thyroid hormone? *Endocrinology* 152, 3259–3267. doi: 10.1210/en.2010-1408
- Küpper, F. C., Carpenter, L. J., Mcfiggans, G. B., Palmer, C. J., Waite, T. J., Boneberg, E. M., et al. (2008). Iodide accumulation provides kelp with an inorganic antioxidant impacting atmospheric chemistry. *Proc. Natl. Acad. Sci. U.S.A.* 105, 6954–6958. doi: 10.1073/pnas.0709959105
- Küpper, F. C., Schweigert, N., Ar Gall, E., Legendre, J.-M., Vilter, H., and Kloareg, B. (1998). Iodine uptake in Laminariales involves extracellular, haloperoxidase-mediated oxidation of iodide. *Planta* 207, 163–171. doi: 10.1007/s004250050469
- La Barre, S., Potin, P., Leblanc, C., and Delage, L. (2010). The halogenated metabolism of brown algae (Phaeophyta), its biological importance and its environmental significance. *Mar. Drugs* 8, 988–1010. doi: 10.3390/md8040988
- Langmead, B., and Salzberg, S. L. (2012). Fast gapped-read alignment with Bowtie 2. *Nat. Methods* 9, 357–359. doi: 10.1038/nmeth.1923
- Laudet, V. (2011). The origins and evolution of vertebrate metamorphosis. *Curr. Biol.* 21, R726–R737. doi: 10.1016/j.cub.2011.07.030
- Leblanc, C., Colin, C., Cosse, A., Delage, L., La Barre, S., Morin, P., et al. (2006). Iodine transfers in the coastal marine environment: the key role of brown algae and of their vanadium-dependent haloperoxidases. *Biochimie* 88, 1773–1785. doi: 10.1016/j.biochi.2006.09.001
- Liu, W. H., Huang, Z. W., Li, P., Xia, J. F., and Chen, B. (2012). Formation of triacylglycerol in *Nitzschia closterium f. minutissima* under nitrogen limitation and possible physiological and biochemical mechanisms. *J. Exp. Mar. Biol. Ecol.* 418, 24–29. doi: 10.1016/j.jembe.2012.03.005
- Lobanov, A. V., Fomenko, D. E., Zhang, Y., Sengupta, A., Hatfield, D. L., and Gladyshev, V. N. (2007). Evolutionary dynamics of eukaryotic selenoproteomes: large selenoproteomes may associate with aquatic life and small with terrestrial life. *Genome Biol.* 8:R198. doi: 10.1186/gb-2007-8-9-r198

- Luo, R., Liu, B., Xie, Y., Li, Z., Huang, W., Yuan, J., et al. (2012). SOAPdenovo2: an empirically improved memory-efficient short-read *de novo* assembler. *Gigascience* 1:18. doi: 10.1186/2047-217X-1-18
- Manchado, M., Michan, C., and Pueyo, C. (2000). Hydrogen peroxide activates the SoxRS regulon *in vivo*. *J. Bacteriol.* 182, 6842–6844. doi: 10.1128/JB.182.23.6842-6844.2000
- Moore, R. M., Webb, M., Tokarczyk, T., and Wever, R. (1996). Bromoperoxidase and iodoperoxidase enzymes and production of halogenated methanes in marine diatom cultures. *J. Geophys. Res.* 101, 20899–20908. doi: 10.1029/96JC01248
- Muñoz-Mérida, A., Viguera, E., Claros, M. G., Trelles, O., and Perez-Pulido, A. J. (2014). Sma3s: a three-step modular annotator for large sequence datasets. *DNA Res.* 21, 341–353. doi: 10.1093/dnares/dsu001
- Murphy, C. D., Moore, R. M., and White, R. L. (2000). Peroxidases from marine microalgae. *J. Appl. Phycol.* 12, 507–513. doi: 10.1023/A:1008154231462
- Orozco, A., Valverde, R. C., Olvera, A., and Garcia, G. C. (2012). Iodothyronine deiodinases: a functional and evolutionary perspective. *J. Endocrinol.* 215, 207–219. doi: 10.1530/JOE-12-0258
- Paris, M., Escriva, H., Schubert, M., Brunet, F., Brtko, J., Ciesielski, F., et al. (2008). Amphioxus postembryonic development reveals the homology of chordate metamorphosis. *Current Biol.* 18, 825–830. doi: 10.1016/j.cub.2008.04.078
- Pevzner, P. A., Tang, H., and Waterman, M. S. (2001). An Eulerian path approach to DNA fragment assembly. *Proc Natl Acad Sci, U.S.A.* 98, 9748–9753. doi: 10.1073/pnas.171285098
- Phatarphekar, A., Buss, J. M., and Rokita, S. E. (2014). Iodotyrosine deiodinase: a unique flavoprotein present in organisms of diverse phyla. *Mol. Biosyst.* 10, 86–92. doi: 10.1039/C3MB70398C
- Qiu, H., Price, D. C., Yang, E. C., Yoon, H. S., and Bhattacharya, D. (2015). Evidence of ancient genome reduction in red algae (Rhodophyta). *J. Phycol.* 51, 624–636. doi: 10.1111/jpy.12294
- Qiu, H., Yoon, H. S., and Bhattacharya, D. (2013). Algal endosymbionts as vectors of horizontal gene transfer in photosynthetic eukaryotes. *Front. Plant Sci.* 4:366. doi: 10.3389/fpls.2013.00366
- Rasdi, N. W., and Qin, J. G. (2015). Effect of N:P ratio on growth and chemical composition of *Nannochloropsis oculata* and *Tisochrysis lutea*. *J. Appl. Phycol.* 27, 2221–2230. doi: 10.1007/s10811-014-0495-z
- Shrivastava, A., Tiwari, M., Sinha, R. A., Kumar, A., Balapure, A. K., Bajpai, V. K., et al. (2006). Molecular iodine induces caspase-independent apoptosis in human breast carcinoma cells involving the mitochondria-mediated pathway. *J. Biol. Chem.* 281, 19762–19771. doi: 10.1074/jbc.M600746200
- Sigaud-Kutner, T. C. S., Neto, A. M. P., Pinto, E., and Colepicolo, P. (2005). Diel activities of antioxidant enzymes, photosynthetic pigments and malondialdehyde content in stationary-phase cells of *Tetraselmis gracilis* (Prasinophyceae). *Aquat. Bot.* 82, 239–249. doi: 10.1016/j.aquabot.2005.02.011
- Sigaud-Kutner, T. C., Pinto, E., Okamoto, O. K., Latorre, L. R., and Colepicolo, P. (2002). Changes in superoxide dismutase activity and photosynthetic pigment content during growth of marine phytoplankters in batch-cultures. *Physiol. Plant.* 114, 566–571. doi: 10.1034/j.1399-3054.2002.1140409.x
- Singh, S. P., Dhakshinamoorthy, R., Jaiswal, P., Schmidt, S., Thewes, S., and Baskar, R. (2014). The thyroxine inactivating gene, type III deiodinase, suppresses multiple signaling centers in *Dictyostelium discoideum*. *Dev. Biol.* 396, 256–268. doi: 10.1016/j.ydbio.2014.10.012
- Surget-Groba, Y., and Montoya-Burgos, J. I. (2010). Optimization of *de novo* transcriptome assembly from next-generation sequencing data. *Genome Res.* 20, 1432–1440. doi: 10.1101/gr.103846.109
- Taylor, E., and Heyland, A. (2017). Evolution of thyroid hormone signaling in animals: non-genomic and genomic modes of action. *Mol. Cell. Endocrinol.* 459, 14–20. doi: 10.1016/j.mce.2017.05.019
- van Bergeijk, S. A., Hernández Javier, L., Heyland, A., Manchado, M., and Cañavate, J. P. (2013). Uptake of iodide in the marine haptophyte *Isochrysis* sp. (T.ISO) driven by iodide oxidation. *J. Phycol.* 49, 640–647. doi: 10.1111/jpy.12073
- van Bergeijk, S. A., Hernandez, L., Zubia, E., and Cañavate, J. P. (2016). Iodine balance, growth and biochemical composition of three marine microalgae cultured under various inorganic iodine concentrations. *Mar. Biol.* 163:107. doi: 10.1007/s00227-016-2884-0
- Venturi, S. (2011). Evolutionary significance of iodine. *Curr. Chem. Biol.* 5, 155–162. doi: 10.2174/187231311796765012
- Venturi, S., and Venturi, M. (1999). Iodide, thyroid and stomach carcinogenesis: evolutionary story of a primitive antioxidant? *Eur. J. Endocrinol.* 140, 371–372. doi: 10.1530/eje.0.1400371
- Verhaeghe, E. F., Fraysse, A., Guerin-Kern, J. L., Wu, T. D., Devés, G., Mioskowski, C., et al. (2008). Microchemical imaging of iodine distribution in the brown alga *Laminaria digitata* suggests a new mechanism for its accumulation. *J. Biol. Inorg. Chem.* 13, 257–269. doi: 10.1007/s00775-007-0319-6
- Wu, T., Shi, X., Zhou, Z., Wang, L., Wang, M., Wang, L., et al. (2012). An iodothyronine deiodinase from *Chlamys farreri* and its induced mRNA expression after LPS stimulation. *Fish Shellfish Immunol.* 33, 286–293. doi: 10.1016/j.fsi.2012.05.011
- Yilancioglu, K., Cokol, M., Pastirmaci, I., Erman, B., and Cetiner, S. (2014). Oxidative stress is a mediator for increased lipid accumulation in a newly isolated *Dunaliella salina* strain. *PLoS ONE* 9:e91957. doi: 10.1371/journal.pone.0091957
- Zámocký, M., Gasselhuber, B., Furtmüller, P. G., and Obinger, C. (2014). Turning points in the evolution of peroxidase-catalase superfamily: molecular phylogeny of hybrid heme peroxidases. *Cell. Mol. Life Sci.* 71, 4681–4696. doi: 10.1007/s00018-014-1643-y
- Zámocký, M., and Obinger, C. (2010). “Molecular phylogeny of heme peroxidases,” in *Biocatalysis Based on Heme Peroxidases*, eds E. Torres and M. Ayala (Berlin: Springer), 7–35.

**Conflict of Interest Statement:** The authors declare that the research was conducted in the absence of any commercial or financial relationships that could be construed as a potential conflict of interest.

Copyright © 2018 Hernández Javier, Benzekri, Gut, Claros, van Bergeijk, Cañavate and Manchado. This is an open-access article distributed under the terms of the Creative Commons Attribution License (CC BY). The use, distribution or reproduction in other forums is permitted, provided the original author(s) and the copyright owner are credited and that the original publication in this journal is cited, in accordance with accepted academic practice. No use, distribution or reproduction is permitted which does not comply with these terms.